Electron Transfer Properties and Hydrogen Peroxide Electrocatalysis of Cytochrome *c* Variants at Positions 67 and 80

Stefano Casalini,[†,‡] Gianantonio Battistuzzi,[†] Marco Borsari,[†] Carlo Augusto Bortolotti,[†] Giulia Di Rocco,[†] Antonio Ranieri,[†] and Marco Sola*[,†,§]

Contribution from the Department of Chemistry, University of Modena and Reggio Emilia, Via Campi 183, I-41100 Modena, Italy, and CNR-INFM National Center nanoStructures and bioSystems at Surfaces - S3, Via Campi 213/A, I-41100 Modena, Italy

Received: September 18, 2009; Revised Manuscript Received: December 18, 2009

Replacement of the axial Met80 heme ligand in electrode-immobilized cytochrome *c* with a noncoordinating Ala residue and alteration of the hydrogen bonding network in the region nearby following substitution of Tyr67 were investigated as effectors of the thermodynamics and kinetics of the protein−electrode electron transfer (ET) and the heme-mediated electrocatalytic reduction of H_2O_2. To this end, the voltammetry of the Met80Ala, Met80Ala/Tyr67His, and Met80Ala/Tyr67Ala variants of yeast iso-1-cytochrome *c* chemisorbed on carboxyalkanethiol self-assembled monolayers was measured at varying temperature and hydrogen peroxide concentration. The thermodynamic study shows that insertion of His and Ala residues in place of Tyr67 results mainly in differences in protein−solvent interactions at the heme crevice with no relevant effects on the $E^{o\prime}$ values at pH 7, which for single and double variants range from approximately −0.200 to −0.220 V (vs SHE). On the contrary, both double variants show much lower ET rates compared to Met80Ala, most likely as a consequence of a change in the ET pathways. In the present nondenaturing immobilizing conditions, and with hydrogen peroxide concentrations in the micromolar range, the variants catalyze H_2O_2 reduction at the electrode, whereas wild-type cytochrome *c* does not. H_2O_2 electrocatalysis occurs with an efficient mechanism likely involving a fast catalase-like process followed by electrocatalytic reduction of the resulting dioxygen at the electrode. Comparison of Met80Ala/Tyr67His with Met80Ala/Tyr67Ala shows that the presence of a general acid−base residue for H_2O_2 recognition and binding through H-bonding in the distal heme site is a key requisite for the reductive turnover of this substrate.

Introduction

Heterogeneous protein−electrode electron transfer (ET) is the fundamental event for the current and potential responses of hybrid interfaces made of self-assembled redox proteins in an electrochemical environment. These constructs can variably be exploited in nanostructured bioelectronic devices, from field effect-like transistors to biosensors.[1−7] In these systems, replacement of large and delicate redox enzymes with small electron-transfer proteins, as are or subjected to a tailored engineering, is an open field of investigation.[8−16] In particular, the advantages offered by modified cytochrome *c* (cytc hereafter) compared to a larger heme-enzyme as the core constituent of an amperometric biosensor for substrates of industrial and clinical importance (such as O_2, O_2^-, H_2O_2, NO, CO, NO_2^-) include: (i) an easier electrical communication between the redox center and the electrode; (ii) the covalent anchoring of the heme to the protein matrix that would prevent heme loss in hostile environments; (iii) the stability of the protein over a wide range of *T* and pH; and (iv) the availability of an easily tunable system to optimize performances.

The problem of hydrogen peroxide biosensing is of particular interest as this molecule is directly related to the level of oxidative stress of cellular and extracellular fluids/compartments.[17] Catalases and peroxidases act as antioxidant protective enzymes as they get rid of hydrogen peroxide utilizing it as an oxidant for useful cellular chemistry or disproportionating it to water and dioxygen, respectively.[18,19] Therefore, their heme site is poised to recognize and turn over hydrogen peroxide. It follows that modification of the heme environment of cytochrome *c* with insertion of some key features of the above sites could lead to an efficient and robust catalytic system for the redox turnover of H_2O_2.[20,21] The basic changes would include removal of the sixth axial iron ligand (Met 80) to produce a five-coordinate heme center, enlargement of the distal cavity, and insertion of a distal histidine.[20] This would help H_2O_2 recognition and binding to the heme center of cytc, and subsequent reduction to water could then be achieved with electrons either provided by a substrate in a conventional peroxidase reaction in solution or delivered through an electrode to an immobilized protein. Here we focus on the latter case, in which the protein would show a "pseudoperoxidase activity", exploitable for amperometric H_2O_2 biosensing.[22] In particular, our aim is to understand how the aforementioned basic changes in the heme site needed for activity affect the redox thermodynamics of cytochrome *c* and the rate of heterogeneous ET. Thus, mutations were made at the axial Met80 heme ligand, which was replaced with a noncoordinating Ala residue and at Tyr67 which was substituted with a His and Ala residue (Figure 1). Tyr67 was chosen because its spatial relationship with the heme group in cytc is similar to that of the catalytically relevant

* Corresponding author. Tel.: +39 059 2055037. Fax: +39 059 373543. URL: http://155.185.2.170/sitiwebgruppi/Sola/homesolagroup2009.html. E-mail: marco.sola@unimore.it.

† University of Modena and Reggio Emilia.

‡ Present address: Istituto per lo Studio dei Materiali Nanostrutturati, ISMN-CNR, Via Gobetti 101, I-40129, Bologna, Italy.

§ CNR-INFM National Center - S3.

10.1021/jp9090365
Published on Web 01/08/2010

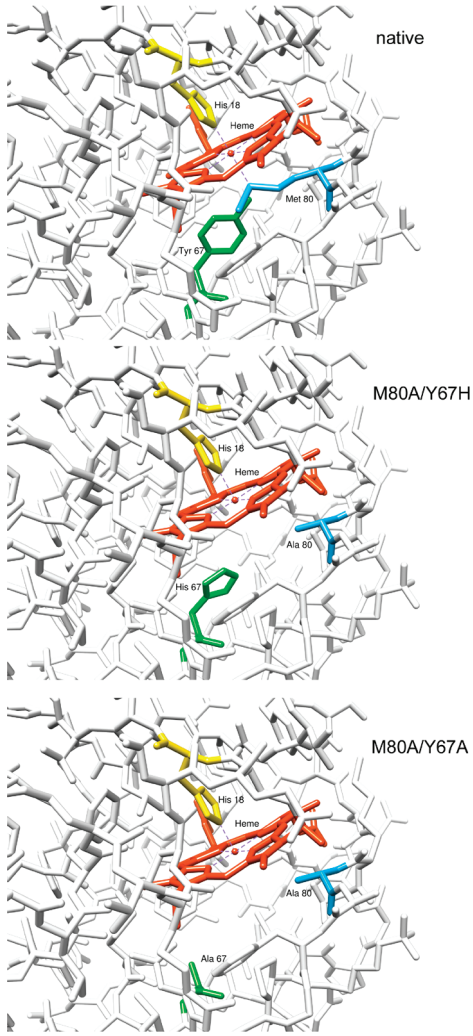

Figure 1. Schematic representations of the heme environment in *Saccharomyces cerevisiae* iso-1-cytochrome *c* and its M80A/Y67H and M80A/Y67A variants. The native cyt *c* representation is based on the X-ray structure (pdb file: 1YCC).[78] The position of the newly introduced residues in the variants has been determined using the UCSF Chimera program,[79] working on the PDB structure of the Y67F mutant of cytochrome *c*.[23] The heme is in red sticks, whereas residues in position 80 and 67 are in blue and green sticks, respectively.

His residue in peroxidases. Moreover, Tyr67 is known to play a key role in maintaining the spatial relationships between several residues at the "distal" heme site in cytc (that of Met80) through a network of hydrogen bond interactions,[23,24] so its mutation (particularly to Ala) would induce changes in the H-bonding, polarity, and dimensions of the distal heme cavity. Moreover, this residue is also involved in the ET route of cytc with redox partners.[25] Following the above, in this work we have investigated the electrochemistry and the electrocatalytic properties toward H_2O_2 of the five-coordinate heme iron-containing single and double variants of yeast iso-1 cytc Met80Ala, Met80Ala/Tyr67His, and Met80Ala/Tyr67Ala. These species were subjected to a nondenaturing electrode immobilization and reacted with micromolar concentrations of H_2O_2 which are known not to affect protein and heme integrity.[26] In this work, we have also considered the mechanistic aspects of the catalytic H_2O_2 reduction at the electrode carried out (or claimed to be) by various heme-containing proteins (cytc at different pH values, microperoxidases, peroxidases) with the aim to clarify, particularly for immobilized *native* cytc,[22] the real nature of the electroactive species. We found that replacement of Tyr67 affects the kinetics of heterogeneous ET of cytc to a much larger extent than the $E^{o\prime}$ value, that *nondenatured* cytc is able to catalytically reduce H_2O_2 only as an engineered five-coordinate heme-containing species, and that the presence of an adequate H-bonding network in the vicinity of the heme iron is a crucial factor for the catalytic activity.

Experimental Methods

Materials. All chemicals were reagent grade. 11-Mercapto-1-undecanoic acid (11-MUAc) and 11-mercapto-1-undecanol (11-MUAl) (Sigma-Aldrich) were recrystallized from hexane before use. Nanopure water was used throughout.

Protein Production and Isolation. The M80A/C102T, M80A/Y67H/C102T, and M80A/Y67A/C102T mutants of untrimethylated recombinant *Saccharomyces cerevisiae* iso-1-cytochrome *c* were produced using the QuikChange XL site-directed mutagenesis kit (Stratagene) starting from the synthetic oligonucleotide primers carrying the desired mutations and using as DNA template the plasmid pMSV1, which had been kindly donated by the late Prof. M. S. Viezzoli of the University of Florence. This plasmid expresses the C102T variant of yeast iso-1-cytochrome *c* from the pTrc promotor and confers ampicillin resistance (cysteine is replaced to avoid dimerization and protein autoreduction). Therefore, all variants considered here contain the C102T mutation. For the sake of simplicity and also because of the lack of functional relevance, this mutation will be omitted in the species designation throughout the paper. It follows that M80A and M80A/Y67H and M80A/Y67A will be referred to as single and double mutants, respectively. Protein expression in *E. coli* and purification were carried out as described elsewhere.[27] Approximately 2 mg of pure protein was obtained from a 1 L culture for both the single and double mutants. The proteins yielded a single band on SDS-PAGE at about 12 kDa, in agreement with the molecular mass calculated from the aminoacidic sequence. The mass spectra for both M80A/Y67A and M80A/Y67H mutants were acquired with a 6410 Triple Quad LC/MS (Agilent Technologies) equipped with an ESI source. The protein concentrations used were 5 μM. The mass spectra obtained are comparable with those for pure cytochrome *c* available in the literature[28] and were used to confirm the molecular mass of the mutants (12 972.35, 12 880.87, and 12 946.25 Da for M80A, M80A/Y67A, and M80A/Y67H, respectively) which resulted to be in agreement with the calculated ones (12 972.45, 12 880.45, and 12 946.55 Da).

The proteins feature an axially bound hydroxide ion at pH above 6.5 (vide infra), with the Soret band maximum at 406 nm.[28−33]

Electrochemical Measurements. A Potentiostat/Galvanostat PAR mod. 273A was used for the cyclic voltammetry (CV) experiments, which were carried out at different scan rates (0.02−10 V s^{-1}) using a three-electrode cell for small volume samples (0.5 mL) under argon. A 1 mm diameter polycrystalline gold wire was used as a working electrode and a Pt sheet and a saturated calomel electrode (SCE) as a counter and reference electrode, respectively. A Vycor (PAR) set ensured the electric contact between the SCE and the working solution. Potentials were calibrated against the MV^{2+}/MV^{+} couple (MV = methylviologen).[34] All the redox potentials reported here are referred to standard hydrogen electrode (SHE). The cleaning procedure for the gold working electrode started with flaming it in oxidizing conditions and subsequent heating in concentrated KOH for 30 min. After rinsing in MILLIQ water, the electrode was dipped in concentrated sulfuric acid for 30 min. To min-

imize residual adsorbed impurities, the electrode was then subjected to 20 voltammetric cycles between +1.5 and −0.25 V at 0.1 V s^{-1} in 1 M H_2SO_4. Finally, it was rinsed in water and anhydrous ethanol. The Vycor set was treated in an ultrasonic pool for about 5 min. Electrode coating with the mixed SAM (self-assembled monolayer) of 11-MUAc/11-MUAl (MUA hereafter) was made by dipping the cleaned electrode into a 1 mM ethanolic 1:1 solution of both substances for 12 h at 5 °C and then rinsing it with MILLIQ water. SAM alignment was achieved performing 10 CV cycles from +0.2 to −0.3 V (vs SCE) with the MUA-coated electrode in a 0.1 M sodium perchlorate solution outgassed with argon. The resulting CV was taken as the background and checked for the absence of spurious signals.

Adsorption of the cytochrome *c* variants on the MUA-coated Au electrode was achieved by dipping the functionalized electrode into a freshly prepared 50 μM protein solution (checked spectrophotometrically) made up in 5 mM phosphate buffer at pH 7, for 24 h at 5 °C. CV experiments on the protein-coated electrodes were performed in 5 mM phosphate buffer containing 5 mM sodium perchlorate at pH 7. The standard reduction potentials ($E^{o\prime}$) of the heme Fe(III)/Fe(II) couple, taken as the average of the anodic and cathodic peak potentials, were invariably found to be reproducible within ± 0.002 V and almost independent of the scan rate in the range 0.01−10 V/s. The pH of the solutions was adjusted with small additions of concentrated HCl or NaOH under fast stirring. To estimate the percentage surface coverage of the protein-coated electrode, the area of the immersed portion of the gold wire was calculated after each CV session by applying the Randles−Sevcik relationship to the CV signal obtained for a solution of ferricinium tetrafluoroborate (an electrochemical standard) using the bare electrode dipped into the standard solution at exactly the same depth of the protein-coated electrode. The electron-transfer rate constants, k_s, for the adsorbed proteins were determined with the method of Laviron,[35] namely, from the change in peak potentials at varying scan rate. The k_s values were averaged over five measurements and found to be reproducible within 10%, which was taken as the associate error.

The reaction entropy for heme Fe(III) to Fe(II) reduction ($\Delta S^{o\prime}_{rc}$) can be determined from variable-temperature $E^{o\prime}$ measurements carried out using a "nonisothermal" electrochemical cell, in which the reference electrode is kept at constant temperature (21 ± 0.1 °C), whereas the half-cell containing the working electrode and the Vycor junction is under thermostatic control[36−38]

$$\Delta S^{o'}_{rc} = S^{o'}_{red} - S^{o'}_{ox} = nF(dE^{o'}/dT) \qquad (1)$$

Thus, $\Delta S^{o\prime}_{rc}$ was determined from the slope of the $E^{o\prime}$ versus T profile which is linear when assuming that $\Delta S^{o\prime}_{rc}$ is constant over the limited temperature range investigated (from 5 to 35 °C). Using the same assumption, the enthalpy change ($\Delta H^{o\prime}_{rc}$) can be obtained from the Gibbs−Helmholtz equation, namely, as the negative slope of the plot of $E^{o\prime}/T$ versus $1/T$. The nonisothermal behavior of the cell was carefully checked by determining the $\Delta H^{o\prime}_{rc}$ and $\Delta S^{o\prime}_{rc}$ values of the ferricyanide/ferrocyanide couple.[37,38] The electrocatalytic reduction of hydrogen peroxide by the immobilized cytc variants was studied by gradually adding aliquots of H_2O_2 solution at known concentration to the O_2-free cell solution at 20 °C.

Results

Proteins. The absorption spectra for oxidized M80A/Y67H and M80A/Y67A at pH 7 (not shown) are identical to that for M80A,[30−32,39,40] indicating that the single and double variants share a low-spin six-coordinate ferric heme iron featuring a hydroxide group bound to the vacant "sixth" axial position.

Electron Transfer and Electrocatalytic Properties. The cyclic voltammograms for M80A/Y67H and M80A/Y67A adsorbed on a polycrystalline MUA-coated Au electrode at pH 7 are shown in Figure 2 along with those for M80A and the wt protein.[42] In all cases, the quasireversible signal (featuring a peak separation of approximately 0.16 V at 20 °C) originates from the one-electron reduction/oxidation of the heme iron of the immobilized protein. As expected, currents increase linearly with scan rate (not shown). These functionalized electrodes are known to not affect appreciably the protein structure of native and mutated cytochromes *c* and to result in small changes in E^o compared to the solution proteins.[41,42] $E^{o\prime}$ values of −0.207 and −0.219 V are obtained at pH 7 for M80A/Y67H and M80A/Y67A, respectively (Table 1). The voltammetric response at pH 7 is persistent for several voltammetric cycles throughout the temperature range investigated. Peak separation increases with increasing scan rate and temperature. However, the $E^{o\prime}$ value is independent of scan rate in the range 0.02−10 V s^{-1}. The surface coverage for the double variants is 16.5 ± 0.8 pmol/cm^2 (corresponding to 87% of a full densely packed monolayer), very similar to that for M80A in the same conditions.[15]

The temperature profiles of $E^{o\prime}$ for M80A,[15] M80A/Y67H, and M80A/Y67A at pH 7 are illustrated in Figure 3. Invariably, the $E^{o\prime}$ values linearly increase with increasing temperature. The reduction thermodynamics are listed in Table 1 along with those for M80A and wt cytc in the same conditions.[15,42]

The rate constants for protein−electrode ET are listed in Table 2, along with the activation enthalpy, calculated from the Arrhenius equation

$$k_s = A' \exp(-\Delta H^{\#}/RT) \qquad (2)$$

i.e., from the slope of the log k_s vs $1/T$ plot (Figure 4). As shown by Bowden et al.,[43−45] the reorganization energy, λ, for the heterogeneous ET can be calculated from the Marcus equation as $\lambda = 4\Delta G^{\#} = 4\Delta H^{\#}$, the activation entropy in these systems being in general negligible.[44,46] The linearized form of the Marcus equation

$$\ln k_s = \ln \nu_0 + [-\beta(r - r_0)] - \Delta G^{\#}/(RT) \qquad (3)$$

allows calculation of the distance of ET between the electrode surface and the heme. As above, $\Delta G^{\#}$ can be assumed to correspond to $\Delta H^{\#}$. A β value of 1 $Å^{-1}$, which is applicable to electron tunneling through the chain of alkane−thiolate carboxylic acids and the protein matrix,[15,44,47,48] and a r_0 value of 3 Å[43,44,49] were used. The estimated tunneling distance is 29.3 and 28.5 Å for M80A/Y67H and M80A/Y67A, respectively. If we consider that the tunneling distance across the chain of MUA is 19 Å,[50,51] the distance from the SAM surface to the heme edge ends up to be 10.3 and 9.5 Å.

The cyclic voltammograms for the immobilized single and double variants, recorded in the presence of increasing micromolar concentrations of hydrogen peroxide at pH 7, are shown in Figure 5. In all cases, the cathodic (anodic) currents progressively increase (decrease) with increasing hydrogen

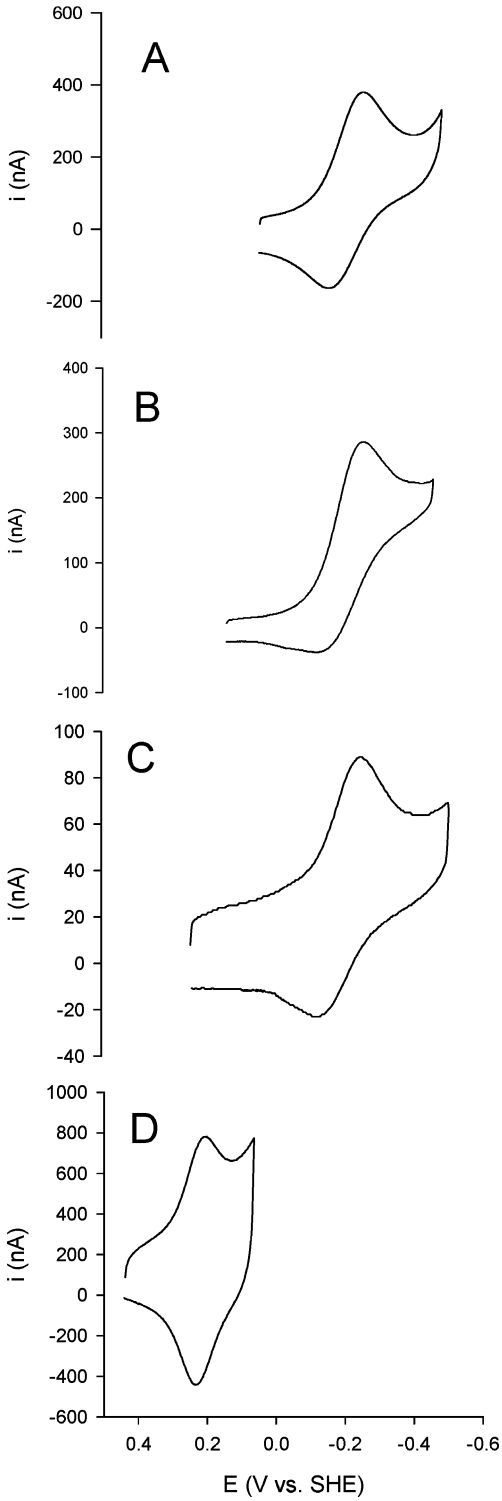

Figure 2. Cyclic voltammograms for the M80A (A), M80A/Y67H (B), and M80A/Y67A (C) variants of *Saccharomyces cerevisiae* iso-1-cytochrome *c* and for the wild-type protein (D) (from ref 42), immobilized on a polycrystalline gold electrode coated with a 1:1 mixed SAM of 11-MUAc and 11-MUAl in 5 mM phosphate buffer, 5 mM sodium perchlorate, pH 7. Sweep rate: 50 mV s^{-1}. $T = 20$ °C.

peroxide concentration, with a typical catalytic behavior, thereby indicating that the adsorbed proteins catalyze H_2O_2 reduction ("pseudoperoxidase" activity).[22] The electrocatalytic effect occurs up to a H_2O_2 concentration of 3 (M80A), 7 (M80A/Y67H), and 18 μM (M80A/Y67A), above which the cathodic currents irreversibly decrease. Below these substrate concentrations limits, elimination of hydrogen peroxide (obtained by rinsing the electrode with buffer) restored the CV signal of the protein; the catalytic currents could then be reobtained upon hydrogen peroxide addition. Therefore, in these conditions the protein layer is stable and reusable. For all variants, no additional peaks

TABLE 1: Thermodynamic Parameters for Fe(III) to Fe(II) Reduction for Single and Double Mutants of *Saccharomyces cerevisiae* Iso-1-cytochrome *c* at Positions 67 and 80 Adsorbed on a Polycrystalline Gold Electrode Coated with a 1:1 Mixed SAM of 11-MUAc and 11-MUAl (MUA)[a]

protein	$E^{o\prime b,c}$ (V)	$\Delta H^{o\prime}{}_{rc}{}^{c}$ (kJ mol^{-1})	$\Delta S^{o\prime}{}_{rc}{}^{c}$ (J K^{-1} mol^{-1})	$-\Delta H^{o\prime}{}_{rc}/F$ (V)	$T\Delta S^{o\prime}{}_{rc}/F^{b}$ (V)
M80A[d]	−0.201	+42	+78	−0.435	+0.241
M80A/Y67H	−0.207	+26	+20	−0.269	+0.062
M80A/Y67A	−0.219	+35	+50	−0.367	+0.154
wt[e]	+0.210	−46	−86	+0.477	−0.266

[a] Values were obtained in 5 mM phosphate buffer, 5 mM sodium perchlorate, at pH 7. [b] Versus SHE, at 298 K. [c] Average errors on $E^{o\prime}$, $\Delta H^{o\prime}{}_{rc}$, and $\Delta S^{o\prime}{}_{rc}$ values are ±0.002 V, ±1 kJ mol^{-1}, and ±2 J mol^{-1} K^{-1}, respectively. [d] From ref 15. [e] From ref 42.

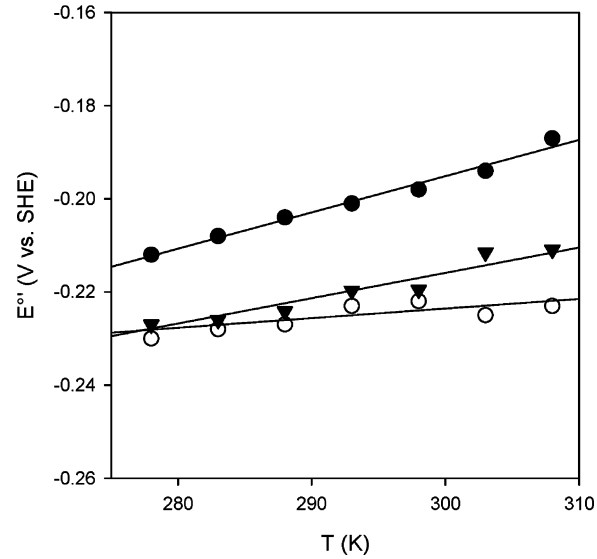

Figure 3. $E^{o\prime}$ vs T plots for the M80A (●), M80A/Y67H (○), and M80A/Y67A (▼) variants of *Saccharomyces cerevisiae* iso-1-cytochrome *c* immobilized on a polycrystalline gold electrode coated with a 1:1 mixed SAM of 11-MUAc and 11-MUAl in 5 mM phosphate buffer and 5 mM sodium perchlorate, pH 7. Solid lines are least-squares fits to the data points. Error bars have the same dimensions of the symbols.

TABLE 2: Kinetic Constants, Activation Enthalpies, and Reorganization Energies for the Protein−Electrode Heterogeneous Electron Transfer for Single and Double Mutants of *Saccharomyces cerevisiae* Iso-1-cytochrome *c* at Positions 67 and 80 Adsorbed on a Polycrystalline Gold Electrode Coated with a 1:1 Mixed SAM of 11-MUAc and 11-MUAl (MUA)[a]

protein	k_s (20 °C)[b] (s^{-1})	$\Delta H^{\#c}$ (kJ mol^{-1})	λ^{c} (eV)	r^{d} (Å)
M80A[e]	1.90	10.8	0.448	7.8
M80A/Y67H	0.23	11.6	0.476	10.3
M80A/Y67A	0.40	11.9	0.492	9.5
wt[f]	46	8.5	0.353	6.5

[a] Values were obtained in 5 mM phosphate buffer and 5 mM sodium perchlorate at pH 7. [b] The relative error on k_s is ±10%. [c] Average errors on $\Delta H^{\#}$ and λ values are ± 0.6 kJ mol^{-1} and ± 0.03 eV, respectively. [d] Distance from the SAM surface to the heme edge (see text). [e] From ref 15. [f] From ref 42.

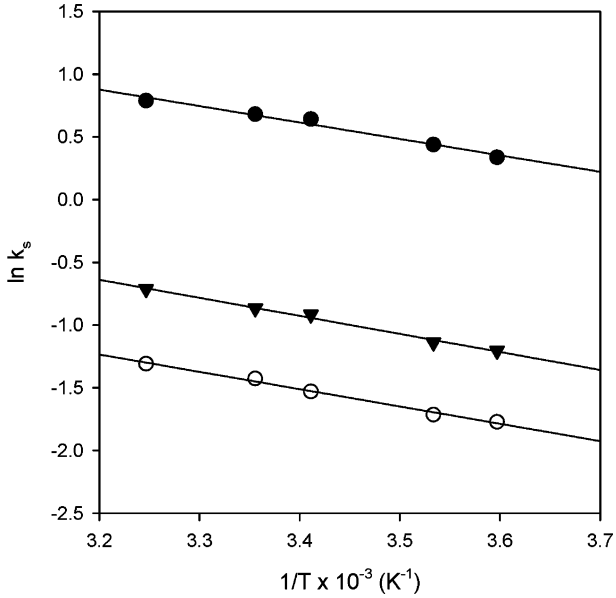

Figure 4. Arrhenius plots for the M80A (●), M80A/Y67H (○), and M80A/Y67A (▼) variants of *Saccharomyces cerevisiae* iso-1-cytochrome *c* immobilized on a polycrystalline gold electrode coated with a 1:1 mixed SAM of 11-MUAc and 11-MUAl in 5 mM phosphate buffer and 5 mM sodium perchlorate, pH 7. Solid lines are least-squares fits to the data points. Error bars have the same dimensions of the symbols.

were detected in the potential range from +0.6 to −0.8 V at all hydrogen peroxide concentrations investigated. In contrast to the variants, immobilized wild-type cytc is unable to carry out the reductive electrocatalysis of hydrogen peroxide. In fact, the CV currents are almost unaffected upon addition of up to 50 μM hydrogen peroxide, above which they progressively and irreversibly decrease.

The catalytic activity of electrode-immobilized cytc variants can be estimated from the Michaelis−Menten equation expressed in terms of current[52]

$$1/i_{cat} = 1/i_{max} + K_M/(i_{max}[H_2O_2]) \quad (4)$$

where i_{cat} is the electrocatalytic current and i_{max} is the maximum current at substrate saturation. The Lineweaver−Burk plots at pH 7, shown in Figure 6, yield the i_{max} and K_M values listed in Table 3. The data indicate that M80A features a larger catalytic efficiency compared to the double mutants.

Discussion

Thermodynamics and Kinetics of Protein−Electrode Electron Transfer. The immobilized single and double cytc variants show very similar $E^{o\prime}$ values at pH 7, which are approximately 400 mV lower than that for wild-type cytc in the same conditions (Table 1).[15,42] The mutation-induced $E^{o\prime}$ decrease can confidently be attributed to the hydroxide ion axially coordinated to the heme iron,[29−33] which stabilizes the ferric heme of the variants, as discussed previously for M80A.[15] Indeed, we have previously shown that the enthalpic stabilization of the oxidized heme in M80A (indicated by a positive $\Delta H^{o\prime}_{rc}$ value) is largely the result of the hard base character of the hydroxide ion which thermodynamically favors the ferric iron.[15] This would also apply to the double mutants (see Table 1). The positive reduction entropy of the variants is consistent with the electrostatically driven increase in the disorder of the water

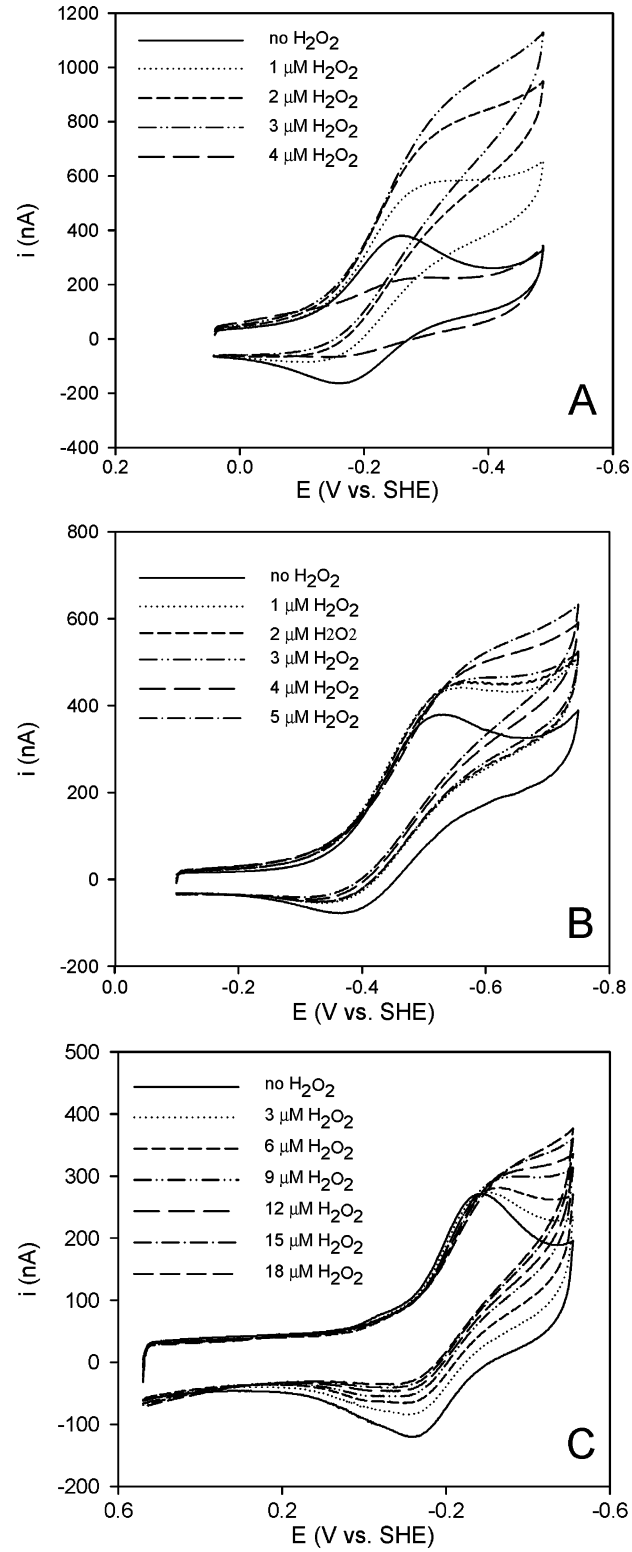

Figure 5. Cyclic voltammograms for the M80A (A), M80A/Y67H (B), and M80A/Y67A (C) variants of *Saccharomyces cerevisiae* iso-1-cytochrome *c* immobilized on a polycrystalline gold electrode coated with a 1:1 mixed SAM of 11-MUAc and 11-MUAl in 5 mM phosphate buffer and 5 mM sodium perchlorate, pH 7, in the presence of increasing concentrations of hydrogen peroxide (indicated in the insets). Sweep rate, 50 mV s^{-1}. T = 20 °C.

molecules in proximity of the heme following the change in the net charge of the heme group from +1 (oxidized) to zero (reduced). A further contribution conceivably arises from the reduction-induced release of the axial hydroxide ligand. As far

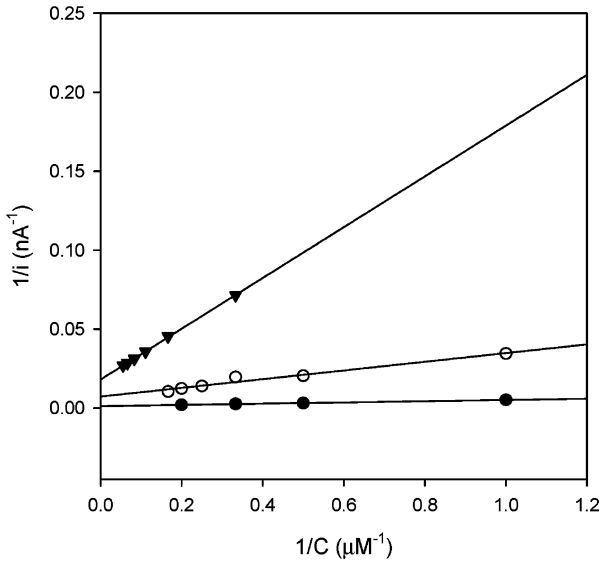

Figure 6. Lineweaver−Burk plot made with the electrocatalytic currents yielded by the M80A (●), M80A/Y67H (○), and M80A/Y67A (▼) variants of *Saccharomyces cerevisiae* iso-1-cytochrome *c* immobilized on a polycrystalline gold electrode coated with a 1:1 mixed SAM of 11-MUAc and 11-MUAl in 5 mM phosphate buffer and 5 mM sodium perchlorate, pH 7, in the presence of increasing concentrations of H_2O_2. Solid lines are least-squares fits to the data points.

TABLE 3: Kinetic Parameters for Electrocatalytic Hydrogen Peroxide Reduction Carried Out by the Single and Double Mutants of *Saccharomyces cerevisiae* Iso-1-cytochrome *c* at Positions 67 and 80 Adsorbed on a Polycrystalline Gold Electrode Coated with a 1:1 Mixed SAM of 11-MUAc and 11-MUAl (MUA)[a]

protein	i_{max}[b] (μA cm^{-2})	K_M[c] (μM)
M80A	9.26	3.25
M80A/Y67H	2.91	3.7
M80A/Y67A	0.94	8.90

[a] Values were obtained in 5 mM phosphate buffer and 5 mM sodium perchlorate at pH 7. [b] The relative error on i_{max} is 8%. [c] The relative error on K_M is 10%.

as the differences in the reduction thermodynamics among the variants are concerned, we have to consider that the reduction enthalpy and entropy of metalloproteins are heavily affected by solvent reorganization effects within the hydration sphere of the molecule.[53−57] These are responsible for the compensatory behavior observed for the $\Delta H^{o\prime}_{rc}$ and $\Delta S^{o\prime}_{rc}$ values within series of homologous proteins, including variants of the same species, differing in the features of the protein−solvent interface.[53−57] Therefore, the changes in reduction thermodynamics due to point mutations are most often masked by these solvent-related effects which, however, owing to their compensatory behavior, do not influence the $E^{o\prime}$ value. We note indeed that M80A/Y67H, M80A/Y67A, and M80A show different $\Delta H^{o\prime}_{rc}$ and $\Delta S^{o\prime}_{rc}$ values whose effects are almost perfectly compensatory, thus resulting in approximately the same $E^{o\prime}$ value. Therefore, it is apparent that insertion of His and Ala residues in place of Tyr67 results mainly in differences in protein−solvent interaction at the heme crevice, with no dramatic structural and electronic effects at the metal center. This is in line with the finding that Tyr67 substitution alters the H-bonding network in the heme crevice influencing temperature-induced conformational transitions.[58] These changes also facilitate access of hydrogen peroxide to the heme site.

The double variants, which lack Tyr67, show ET rate constants which, independently of temperature, are approximately five times (M80A/Y67A) and ten times (M80A/Y67H) lower than that for M80A and 2 orders of magnitude lower than wt cytc in the same conditions (Table 2). We note that the scarce efficiency of the heterogeneous ET for these species is related to both a larger activation barrier and an increased electron donor−acceptor distance. In particular, activation enthalpy and ET distance increase in the order: wt < M80A < double variants (Table 2). The larger $\Delta H^{\#}$ and λ values for M80A with respect to wt cytc were attributed previously to the reduction-induced dissociation of the axial hydroxide ligand.[15] In the double variants, replacement of Tyr67 further raises the energy barrier of the ET process. This effect can be put in relation with the mutation-induced alteration of the local protein conformation[58] and hydrogen bonding network which involved Tyr67 and the sixth axial heme iron ligand (the Met residue and the hydroxide ion in wt and M80A cytc, respectively), the side chains of nearby residues, and the conserved "catalytic" water molecule.[23,24] The large tunneling distance for the double variants cannot be explained unambiguously with the data at hand. Since both mutations are likely not to affect the electrostatic potential of the protein, this distance increase is reasonably not a result of an altered protein−SAM interaction but possibly a consequence of a change in the ET pathway within the heme site subjected to the above-mentioned changes in H-bonding. These observations suggest that the H-bonding network involving Tyr67 facilitates heterogeneous ET, in keeping with the suggested involvement of Tyr67 in the ET pathway of bacterial cytc with redox partners in solution.[25]

H_2O_2 Turnover. The immobilized single and double variants yield electrocatalytic waves for H_2O_2 reduction at pH 7 (Figure 5), whereas wt cytc cannot (in the micromolar range of H_2O_2 concentration studied). The irreversible loss of catalytic activity of the protein layer upon increasing H_2O_2 concentration above a certain threshold (from 3 to 18 μM) can be attributed to the oxidative damage of the protein and destruction of the heme group with loss of iron due to excess hydrogen peroxide, as shown elsewhere for cytochrome *c* in solution.[26] Therefore, at the low H_2O_2 concentrations employed here, the observed electrocatalysis arises from nondenatured proteins, as also testified by the reproducibility of the CV responses of the functionalized electrodes put in the same conditions after having been rinsed with buffer.

The currents follow a Michaelis−Menten behavior (Figure 6), and most importantly, no potential change occurs upon hydrogen peroxide addition in the concentration range investigated. This indicates that, in these conditions, the catalytic form which binds and reduces the substrate is the product of cytcFe(III)−OH^- reduction, namely, the five-coordinate ferrous heme. In this respect, the behavior of the present cytc variants is similar to that of denatured cytochrome *c* at pH 3[59] but differs from that of microperoxidase-11,[60−63] in which a potential shift does occur (toward positive potentials) likely as a result of the formation of the catalytically active Fe(IV) intermediate species in the presence of H_2O_2.[64,65] Therefore, the mechanism of hydrogen peroxide electrocatalysis carried out by the present five-cooordinate heme-containing species at the observed potentials must *not* involve formation of the iron(IV)-oxoporphyrin cation intermediate at the electrode. We note that a simple "Fe^{2+}/Fe^{3+}-only" mechanism, which would be consistent with the observed potential invariance

$$(1)\ \text{cytFe(III)}-OH^- + e^- + H^+ \rightarrow \text{cytFe(II)} + H_2O$$

$$(2)\ \text{cytFe(II)} + H_2O_2 \rightarrow \text{cytFe(III)}{-}OH^- + OH^{\bullet}$$

must be considered extremely improbable at best because of the low affinity of peroxide for the ferrous heme. In fact, the competent oxidation state of the heme iron for H_2O_2 binding and reduction is the ferric state (with oxidation of the metal to the oxoferryl(IV) state), as indicated by the chemistry of peroxidases and microperoxidases.[18,19,64−66] A more complex mechanism can be proposed which accounts for the ferrous heme of the immobilized cytc variants serving as the electrocatalytic reducing center. The chemistry would involve an initial fast catalase-like cycle (steps 1 and 2) (here, the lifetime of the ferryl group of compound I is too short to be detected in the CV experiments with the scan rates employed) resulting in the production of molecular oxygen, which would then undergo a catalytic one-electron reduction at the electrode with production of a superoxide anion (steps 3−5) (the superoxide anion, at these negative working potentials, cannot be reoxidized back to dioxygen by the heme group)

$$(1)\ \text{cytFe(III)}{-}OH^- + H_2O_2 + H^+ \rightarrow \text{compound I} + 2H_2O$$

$$(2)\ \text{compound I} + H_2O_2 \rightarrow \text{cytFe(III)}{-}OH^- + O_2 + H^+$$

$$(3)\ \text{cytFe(III)}{-}OH^- + e^- + H^+ \rightarrow \text{cytFe(II)} + H_2O \quad \text{at electrode}$$

$$(4)\ \text{cytFe(II)} + O_2 \rightarrow \text{cytFe(III)}{-}O_2^-$$

$$(5)\ \text{cytFe(III)}{-}O_2^- + H_2O \rightarrow \text{cytFe(III)}{-}OH^- + H^+ + O_2^-$$

Step 4 would correspond to formation of the enzyme−substrate adduct which, within a Michaelis−Menten model, represents the rate-limiting step of the process, accompanied by fast intramolecular ET. This mechanism parallels that suggested previously for hemoglobin and HRP in the absence of substrates and with excess hydrogen peroxide.[67,68]

The absence of catalytic activity for adsorbed wt cytochrome *c* at these low, nondenaturing, H_2O_2 concentrations indicates that the electrocatalytic activity of the electrode-immobilized native cytochrome *c* in the presence of millimolar H_2O_2 concentration previously investigated[22,60,61,69] cannot be due to the intact protein but to species subjected to an oxidative damaging by hydrogen peroxide, resulting in an altered axial heme coordination (and even heme loss/disruption).[26] Native cytc indeed features a six-coordinate heme iron which is therefore not available, especially in the ferrous state (which strongly binds to the thioether sulfur of the methionine ligand) for substrate binding and reductive turnover.

It is worthy of note that the K_M values of the present cytc variants are in the micromolar range (Table 3). Therefore, the kinetic affinity of H_2O_2 for the heme iron of these species turns out to be from one to three orders larger than those for immobilized horseradish peroxidase,[70−72] hemoglobin variably immobilized on SAM-coated electrodes,[67,70,73−75] microperoxidase 11,[60−63] and wt cytochrome *c* covalently attached to mixed carboxylic acid and hydroxyl-terminated SAM-coated electrodes at low pH,[59] incorporated in a clay,[69] covalently linked to thiopropionic acid-modified electrodes,[61] and immobilized on colloidal gold-modified carbon paste electrode.[22] For immobilized wt cytochrome *c*, we note a great variability of the K_M values reported in the literature. This is likely the result of a different degree of cytc degradation due to H_2O_2, influenced by the immobilization procedure, which affects the nature and the population of the electroactive species.

We observe that the electrocatalytic activity of both double variants toward hydrogen peroxide reduction is lower than that of M80A cytc which indeed shows the largest affinity for the substrate and the largest currents (Table 3). In particular, the catalytic efficiency follows the order: M80A ≫ M80A/Y67H > M80A/Y67A. The replacement of Tyr67 with a His and an Ala residue increases the dimensions of an already existing heme cavity near Tyr67 and the accessibility of the heme group to solvent and substrate.[23] However, this effect turns out to depress the catalytic efficiency, particularly when coupled, in the M80A/Y67A variant, with the decrease in polarity and H-bonding properties of the heme crevice. Thus, apparently, the presence of a site capable of establishing an H-bond with the hydrogen peroxide molecule (or hydroperoxide anion) is a crucial feature for molecular recognition and reductive turnover.

The data presented here cannot be compared easily with the recently determined kinetics of guaiacol oxidation carried out in solution by the M80V, Y67H, and M80V/Y67H cytc variants.[20] This is mainly because the reaction is not the same; in fact, here we deal with a "pseudoperoxidase" activity involving H_2O_2 reduction carried out by an electrode-immobilized protein and not with a conventional peroxidase reaction involving a solution protein and a reducing substrate. The order of the peroxidase efficiency of the above cytc variants was found to be: Y67H ≫ M80V/Y67H > M80V ≫ wt. Therefore, apparently the presence of His67 acting as a general acid−base catalyst for H_2O_2 leading to the formation of compound I in the peroxidase cycle is more important than the absence of the endogenous "sixth" axial heme iron ligand for the enzymatic activity of engineered cytc.[20] We note that for the peroxidase reaction the presence of a certain catalytic activity also for wt cytc is more plausible than the pseudoperoxidase activity mentioned above. In fact, formation of compound I requires that H_2O_2 reacts with Fe(III), which features a rather low affinity for the thioether sulfur of the Met ligand, which could therefore be displaced by H_2O_2 in an at least partially unfolded species.[76,77] We believe that the results for the cytc variants in solution and the present data can be considered in agreement. Both indeed highlight the importance of a general acid−base residue being available for H_2O_2 recognition and binding. This, for the peroxidase reaction in solution, prevails over the absence of the sixth protein axial ligand (likely because the five-coordinate heme iron already exists as a result of H_2O_2-induced protein unfolding), whereas for the pseudoperoxidase reaction it overcomes the effects of a larger accessibility of the heme crevice.

Conclusions

The differences in the H-bonding network in the heme crevice between the electrode-immobilized M80A variant of yeast iso-1-cytochrome *c* and the double variants M80A/Y67H and M80A/Y67A originate modest $E^{o\prime}$ changes due to enthalpy−entropy compensation effects. Substitution of Tyr67 instead depresses the kinetics of the protein−electrode

electron transfer. This residue therefore results to be involved in the heterogeneous ET pathway. Moreover, the absence of the sixth axial heme ligand in cytochrome *c* turns out to be an essential requisite for the intact protein to act as an immobilized electrocatalyst of H_2O_2 reduction, which most likely proceeds through the reductive catalysis of dioxygen produced by an initial catalase-like process. The data for the M80A/Y67H and M80A/Y67A variants indicate that the presence of a general acid−base residue for H_2O_2 recognition and binding through H-bonding is a key requisite for reductive substrate turnover. Moreover, the catalytic efficiency of these cytochrome *c* variants turns out to be much larger than that of immobilized HRP, microperoxidase-11, hemoglobin, and myoglobin and is characterized by a good signal durability. These hybrid interfaces thereby result to be good candidates as core constituents of H_2O_2 sensing devices.

Acknowledgment. This work was supported by the Ministero dell'Università e della Ricerca (MUR) of Italy (Programmi di Ricerca Scientifica di Rilevante Interesse Nazionale 2007 Prot. n. 2007KAWXCL and n. 20079Y9578), by the Fondazione Cassa di Risparmio di Modena (progetto Prot. N. 1297.08.8C), and by the Università di Modena e Reggio Emilia (Fondo di Ateneo per la Ricerca, 2007). Molecular graphics images were produced using the UCSF Chimera package from the Resource for Biocomputing, Visualization, and Informatics at the University of California, San Francisco (supported by NIH P41 RR-01081). LC-MS measurements were carried out at the Centro Grandi Strumenti of the University of Modena and Reggio Emilia. The personnel is gratefully acknowledged for assistance.

References and Notes

(1) Willner, I.; Basnar, B.; Willner, B. *FEBS J.* **2007**, *274*, 302–309.
(2) Willner, I.; Katz, E. *Angew. Chem., Int. Ed.* **2000**, *39*, 1180–1218.
(3) Murphy, L. *Curr. Opin. Chem. Biol.* **2006**, *10*, 177–184.
(4) Zhang, W.; Li, G. *Anal. Sci.* **2004**, *20*, 603–609.
(5) Göpel, W.; Heiduschka, P. *Biosens. Bioelectron.* **1995**, *10*, 853–883.
(6) Alessandrini, A.; Salerno, M.; Frabboni, S.; Facci, P. *Appl. Phys. Lett.* **2005**, *86*, 133902.
(7) Rinaldi, R.; Biasco, A.; Maruccio, G.; Arima, V.; Visconti, P.; Cingolani, R.; Facci, P.; De Rienzo, F.; Di Felice, R.; Molinari, E.; Veerbeet, M. Ph.; Canters, G. W. *Appl. Phys. Lett.* **2003**, *82*, 472–474.
(8) Wegerich, F.; Turano, P.; Allegrozzi, M.; Möhwald, H.; Lisdat, F. *Anal. Chem.* **2009**, *81*, 2976–2984.
(9) Scheller, W.; Jin, W.; Ehrentreich-Forster, E.; Ge, B.; Lisdat, F.; Buttemeier, R.; Wollenberger, U.; Scheller, F. W. *Electroanalysis* **1999**, *11*, 703–706.
(10) Lisdat, F.; Ge, B.; Ehrentreich-Forster, E.; Reszka, R.; Scheller, F. W. *Anal. Chem.* **1999**, *71*, 1359–1365.
(11) Ignatov, S.; Shishniashvili, D.; Ge, B.; Scheller, F. W.; Lisdat, F. *Biosens. Bioelectron.* **2002**, *17*, 191–199.
(12) Lu, Y.; Berry, S. M.; Pfister, T. D. *Chem. Rev.* **2001**, *101*, 3047–3080.
(13) Ozaki, S.-I.; Roach, M. P.; Matsui, T.; Watanabe, Y. *Acc. Chem. Res.* **2001**, *34*, 818–825.
(14) Bortolotti, C. A.; Battistuzzi, G.; Borsari, M.; Facci, P.; Ranieri, A.; Sola, M. *J. Am. Chem. Soc.* **2006**, *128*, 5444–5451.
(15) Casalini, S.; Battistuzzi, G.; Borsari, M.; Bortolotti, C. A.; Ranieri, A.; Sola, M. *J. Phys. Chem. B* **2008**, *112*, 1555–1563.
(16) Casalini, S.; Battistuzzi, G.; Borsari, M.; Ranieri, A.; Sola, M. *J. Am. Chem. Soc.* **2008**, *130*, 15099–15104.
(17) Halliwell, B.; Clement, M. V.; Long, L. H. *FEBS Lett.* **2000**, *486*, 10–13.
(18) Zederbauer, M.; Furtmüller, P. G.; Brogioni, S.; Jakopitsch, C.; Smulevich, G.; Obinger, C. *Nat. Prod. Rep.* **2007**, *24*, 571–584.
(19) Chelikani, P.; Fita, I.; Loewen, P. C. *Cell. Mol. Life Sci.* **2004**, *61*, 192–208.
(20) Wang, Z.-H.; Lin, Y.-W.; Rosell, F. I.; Ni, F.-Y.; Lu, H.-J.; Yang, P.-Y.; Tan, X.-S.; Li, X.-Y.; Huang, Z.-X.; Mauk, A. G. *ChemBioChem* **2007**, *8*, 607–609.
(21) Diederix, R. E.; Ubbink, M.; Canters, G. W. *Eur. J. Biochem.* **2001**, *268*, 4207–4216.
(22) Ju, H.; Liu, S.; Ge, B.; Lisdat, F.; Scheller, F. W. *Electroanalysis* **2002**, *14*, 141–147.
(23) Berghuis, A. M.; Guillemette, J. G.; Smith, M.; Brayer, G. D. *J. Mol. Biol.* **1994**, *235*, 1326–1341.
(24) Berghuis, A. M.; Guillemette, J. G.; McLendon, G.; Sherman, F.; Smith, M.; Brayer, G. D. *J. Mol. Biol.* **1994**, *236*, 786–799.
(25) Sebban-Kreuzer, C.; Blackledge, M.; Dolla, A.; Marion, D.; Guerlesquin, F. *Biochemistry* **1998**, *37*, 8331–8340.
(26) Villegas, J. A.; Mauk, A. G.; Vazquez-Duhalt, R. *Chem. Biol.* **2000**, *7*, 237–244.
(27) Barker, P. D.; Bertini, I.; Del Conte, R.; Ferguson, S. J.; Hajieva, P.; Tomlinson, E.; Turano, P.; Viezzoli, M. S. *Eur. J. Biochem.* **2001**, *268*, 4468–4476.
(28) Liu, J.; Konermann, L. *J. Am. Soc. Mass. Spectrom.* **2009**, *20*, 819–828.
(29) Banci, L.; Bertini, I.; Bren, K. L.; Gray, H. B.; Turano, P. *Chem. Biol.* **1995**, *2*, 377–383.
(30) Banci, L.; Bertini, I.; Bren, K. L.; Gray, H. B.; Sompornpisut, P.; Turano, P. *Biochemistry* **1995**, *34*, 11385–11398.
(31) Lu, Y.; Casimiro, D. R.; Bren, K. L.; Richards, J. H.; Gray, H. B. *Proc. Natl. Acad. Sci. U.S.A.* **1993**, *90*, 11456–11459.
(32) Bren, K. L.; Gray, H. B. *J. Am. Chem. Soc.* **1993**, *115*, 10382–10383.
(33) Bren, K. L.; Gray, H. B. *J. Inorg. Biochem.* **1993**, *51*, 111.
(34) Battistuzzi, G.; Borsari, M.; Ranieri, A.; Sola, M. *Arch. Biochem. Biophys.* **2002**, *404*, 227–233.
(35) Laviron, E. *J. Electroanal. Chem.* **1979**, *101*, 19–28.
(36) Yee, E. L.; Cave, R. J.; Guyer, K. L.; Tyma, P. D.; Weaver, M. J. *J. Am. Chem. Soc.* **1979**, *101*, 1131–1137.
(37) Yee, E. L.; Weaver, M. J. *Inorg. Chem.* **1980**, *19*, 1077–1079.
(38) Taniguchi, V. T.; Sailasuta-Scott, N.; Anson, F. C.; Gray, H. B. *Pure Appl. Chem.* **1980**, *52*, 2275–2281.
(39) Silkstone, G. G.; Cooper, C. E.; Svistunenko, D.; Wilson, M. T. *J. Am. Chem. Soc.* **2005**, *127*, 92–99.
(40) Silkstone, G. G.; Stanway, G.; Brzezinski, P.; Wilson, M. T. *Biophys. Chem.* **2002**, *98*, 65–77.
(41) Dick, L. A.; Hanes, A. J.; Van Duyne, R. P. *J. Phys. Chem. B* **2000**, *104*, 11752–11762.
(42) Battistuzzi, G.; Bortolotti, C. A.; Borsari, M.; Di Rocco, G.; Ranieri, A.; Sola, M. *J. Phys. Chem. B* **2007**, *111*, 10281–10287.
(43) Tarlov, M. J.; Bowden, E. F. *J. Am. Chem. Soc.* **1991**, *113*, 1847–1849.
(44) Song, S.; Clark, R. A.; Bowden, E. F.; Tarlov, M. J. *J. Phys. Chem.* **1993**, *97*, 6564–6572.
(45) Nahir, T. M.; Clark, R. A.; Bowden, E. F. *Anal. Chem.* **1994**, *66*, 2595–2598.
(46) Weaver, M. J. *J. Phys. Chem.* **1979**, *13*, 1748–1757.
(47) Becka, A. M.; Miller, C. J. *J. Phys. Chem.* **1992**, *96*, 2657–2668.
(48) Finklea, H. O.; Hanshew, D. D. *J. Am. Chem. Soc.* **1992**, *114*, 3173–3181.
(49) Marcus, R. A.; Sutin, N. *Biochim. Biophys. Acta* **1985**, *811*, 265–322.
(50) Murgida, D. H.; Hildebrandt, P. *J. Phys. Chem. B* **2001**, *105*, 1578–1586.
(51) Hildebrand, P.; Murgida, D. H. *Bioelectrochemistry* **2002**, *55*, 139–143.
(52) Kamin, R. A.; Willson, G. S. *Anal. Chem.* **1980**, *52*, 1198–1205.
(53) Grunwald, E.; Steel, C. *J. Am. Chem. Soc.* **1995**, *117*, 5687–5692.
(54) Liu, L.; Guo, Q.-X. *Chem. Rev.* **2001**, *101*, 673–695.
(55) Lumry, R.; Rajender, S. *Biopolymers* **1970**, *9*, 1125–1127.
(56) Battistuzzi, G.; Borsari, M.; Sola, M. *Chemtracts - Inorg. Chem.* **2005**, *18*, 73–86.
(57) Battistuzzi, G.; Borsari, M.; Di Rocco, G.; Ranieri, A.; Sola, M. *J. Biol. Inorg. Chem.* **2004**, *9*, 23–26.
(58) Ying, T.; Wang, Z.-H.; Lin, Y.-W.; Xie, J.; Tan, X.; Huang, Z.-X. *Chem. Commun.* **2009**, 4512–4514.
(59) Wang, L.; Waldeck, D. H. *J. Phys. Chem. C* **2008**, *112*, 1351–1356.
(60) Lötzbeyer, T.; Schuhmann, W.; Schmidt, H.-L. *J. Electronal. Chem.* **1995**, *395*, 339–343.
(61) Lötzbeyer, T.; Schuhmann, W.; Schmidt, H.-L. *Sens. Actuators, B* **1996**, *33*, 50–54.
(62) Huang, W.; Jia, J.; Zhang, Z.; Han, X.; Tang, J.; Wang, J.; Dong, S.; Wang, E. *Biosens. Bioelectron.* **2003**, *18*, 1225–1230.
(63) Moore, A. N. J.; Katz, E.; Willner, I. *J. Electroanal. Chem.* **1996**, *417*, 189–192.
(64) Traylor, T. G.; Xu, F. *J. Am. Chem. Soc.* **1990**, *112*, 178–186.
(65) Baldwin, D. A.; Marques, H. M.; Pratt, J. M. *J. Inorg. Biochem.* **1987**, *30*, 203–217.
(66) Adams, P. A.; Goold, R. D. *J. Chem. Soc., Chem. Commun.* **1990**, 97–98.

(67) Huang, R.; Hu, N. *Bioelectrochemistry* **2001**, *54*, 75–81.
(68) He, P.; Hu, N.; Zhou, G. *Biomacromolecules* **2002**, *3*, 139–146.
(69) Lei, C. H.; Lisdat, F.; Wollenberger, U.; Scheller, F. W. *Electroanalysis* **1999**, *11*, 274–276.
(70) Li, D. J.; Tian, S. N.; Ge, H. *Anal. Chim. Acta* **1996**, *335*, 137–145.
(71) Qian, J.; Liu, Y.; Liu, H.; Yu, T.; Deng, J. *J. Electroanal. Chem.* **1995**, *397*, 157–162.
(72) Xiao, Y.; Ju, H. X.; Chen, H. Y. *Anal. Biochem.* **2000**, *278*, 22–28.
(73) Zhao, Y.-D.; Bi, Y.-H.; Zhang, W.-D.; Luo, Q.-M. *Talanta* **2005**, *65*, 489–494.
(74) Fan, C.; Wang, H.; Sun, S.; Zhu, D.; Wagner, G.; Li, G. *Anal. Chem.* **2001**, *73*, 2850–2854.
(75) Tong, Z.; Yuan, R.; Chai, Y.; Chen, S.; Xie, Y. *Thin Solid Films* **2007**, *515*, 8054–8058.
(76) Diederix, R. E.; Ubbink, M.; Canters, G. W. *ChemBioChem* **2002**, *3*, 110–112.
(77) Basova, L. V.; Kurnikov, I. V.; Wang, L.; Rotov, V. B.; Belikova, N. A.; Vlasova, I. I.; Pacheco, A. A.; Winnica, D. E.; Peterson, J.; Bayir, H.; Waldeck, D. H.; Kagan, V. E. *Biochemistry* **2007**, *46*, 3423–3434.
(78) Louie, G. V.; Brayer, G. D. *J. Mol. Biol.* **1990**, *214*, 527–555.
(79) Pettersen, E. F.; Goddard, T. D.; Huang, C. C.; Couch, G. S.; Greenblatt, D. M.; Meng, E. C.; Ferrin, T. E. *J. Comput. Chem.* **2004**, *25*, 1605–1612.

JP9090365